

Majorana Component in the Imaginary Potential for $p + \alpha$ Scattering*

D. R. Thompson, Y. C. Tang, and Ronald E. Brown

School of Physics, University of Minnesota, Minneapolis, Minnesota 55455

(Received 3 February 1972)

A phenomenological, imaginary potential is incorporated into resonating-group calculations for the $p + \alpha$ system. The introduction of this potential allows, at energies above the reaction threshold of 18.35 MeV (c.m.), a more detailed comparison with experiment than was possible with previous resonating-group calculations. The calculations are compared with elastic scattering differential-cross-section data, polarization data, and spin-rotation-parameter data which exist between 23 and 75 MeV (c.m.). From this comparison it is concluded that a Majorana component whose strength varies with energy is very likely present in the imaginary potential.

I. INTRODUCTION

In the present study we investigate the consequences of the inclusion of a phenomenological imaginary potential in resonating-group calculations for the $p + \alpha$ system, the purpose being to account approximately for the influence of reactions on the elastic channel. Previous resonating-group calculations for this system have been reported¹ in which a spin-orbit component was included in the employed nucleon-nucleon potential, but which did not attempt to take into account reaction effects. In those calculations good agreement with the experimental elastic scattering differential cross sections and polarizations was obtained at energies up to several MeV above the reaction threshold of 18.35 MeV.² This agreement indicates that the real part of the $p + \alpha$ interaction is given reasonably well by a one-channel, resonating-group calculation, and consequently, when a phenomenological absorptive potential is added, there are expected to be no complications arising from possible gross uncertainties in the real part of the interaction. Therefore, it can reasonably be hoped that many of the features of the $p + \alpha$ imaginary potential revealed by the present study are basically correct. Furthermore, some success has recently been attained in the investigation of other systems³⁻⁵ by this method.

The present work consists of the application of the theory to the fitting of elastic scattering differential-cross-section data, polarization data, and spin-rotation-parameter data in the energy range 23 to 75 MeV. Except for some discrepancies in the forward-angle polarizations, the fits are quite good. To reproduce the data it was found necessary to include a Majorana (space-exchange) component in the imaginary potential. As will be discussed in Sec. III, such a feature of the imaginary potential is not entirely unexpected.

In Sec. II a brief formulation of the theory is given, and in Sec. III the absorptive potential is discussed and the rationale for the inclusion of a Majorana component is presented. The results of our study are presented in Sec. IV, and in Sec. V a discussion and conclusions are given.

II. FORMULATION

The formulation of the $p + \alpha$ problem using the resonating-group method is discussed in Ref. 1, and the full details will not be repeated here. The method employs a five-particle Hamiltonian operator with a nucleon-nucleon potential containing a spin-orbit interaction and containing a central interaction with a space-exchange component and with different ranges in the spin-singlet and spin-triplet states. A completely antisymmetrized, five-particle trial wave function of a $p + \alpha$ cluster type is used along with the Hamiltonian operator in a variational calculation of the radial function $f_{Jl}(r)$, where r is the distance between the proton p and the c.m. of the α cluster, l is the $p + \alpha$ relative orbital angular momentum, and J is the total angular momentum of the system. This variational calculation leads to Eq. (8) of Ref. 1, which is an integrodifferential equation for $f_{Jl}(r)$. Upon the addition of a phenomenological imaginary potential iW to the theory, this integrodifferential equation can be written in the form

$$\left[\frac{\hbar^2}{2\mu} \left(\frac{d^2}{dr^2} - \frac{l(l+1)}{r^2} \right) + E - V_{Jl}(r) - iW_{Jl}(r) \right] f_{Jl}(r) = \int_0^\infty k_{Jl}(r, r') f_{Jl}(r') dr', \quad (1)$$

where we have explicitly allowed for the possibility of a (J, l) dependence in the absorptive potential $iW_{Jl}(r)$. In Eq. (1), μ is the reduced mass of

the $p+\alpha$ system, E is the total kinetic energy in the c.m. system at large p - α separation, and the potential $V_N(r)$ and the kernel $k_N(r, r')$ are derived from the resonating-group method, and expressions for them are given in Ref. 1.

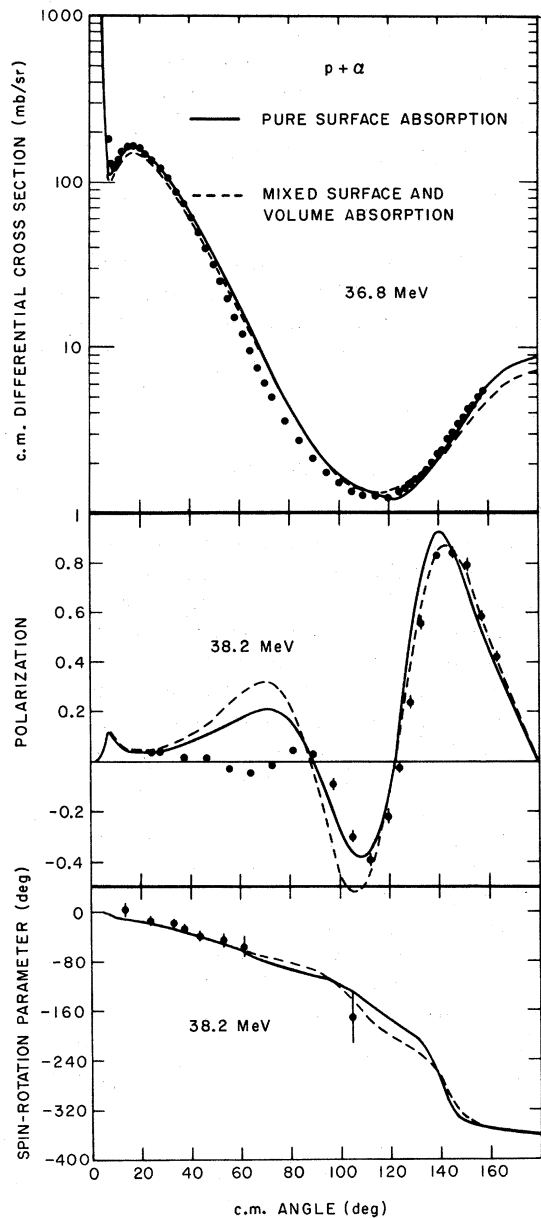


FIG. 1. Comparison of the present calculations with data (points) of Refs. 10-12 at the indicated c.m. energies. The exchange parameter C_I in the absorptive potential has the value -0.7 for both curves. The solid curve represents a calculation with pure surface absorption having parameters $R=2.6$ F, $a=0.2$ F, $U_V=0$, $U_S=5.5$ MeV. The dashed curve represents a calculation with equal surface and volume absorption having parameters $R=2.25$ F, $a=0.5$ F, $U_V=U_S=1.5$ MeV.

From the numerical solution of Eq. (1) for $f_N(r)$, the complex phase shifts $\delta_N = \delta_N^R + i\delta_N^I$ are determined, and from these the scattering amplitudes $g(\theta)$ and $h(\theta)$ are found from the following relations:

$$g(\theta) = f_C(\theta) + \frac{1}{2ik} \sum_l [(l+1)(S_l^+ - 1) + l(S_l^- - 1)] \times e^{2i\sigma_l} P_l(\cos\theta), \quad (2)$$

$$h(\theta) = \frac{1}{2k} \sum_l (S_l^+ - S_l^-) e^{2i\sigma_l} \sin\theta \frac{dP_l(\cos\theta)}{d(\cos\theta)}. \quad (3)$$

Here $f_C(\theta)$ is the Coulomb amplitude, the σ_l are the Coulomb phase shifts, and

$$S_l^+ \equiv S_{l+\frac{1}{2}, l}, \quad S_l^- \equiv S_{l-\frac{1}{2}, l}, \quad (4)$$

with

$$S_N \equiv e^{2i\delta_N}. \quad (5)$$

The total reaction cross section σ_R is calculated from

$$\sigma_R = \frac{\pi}{k^2} \sum_l [(l+1)(1 - |S_l^+|^2) + l(1 - |S_l^-|^2)]. \quad (6)$$

Finally, one can obtain from the scattering amplitudes the following expressions for the differential cross section $\sigma(\theta)$, the polarization $P(\theta)$, and the spin-rotation parameter $\beta(\theta)$:

$$\sigma(\theta) = |g(\theta)|^2 + |h(\theta)|^2, \quad (7)$$

$$P(\theta) = 2 \operatorname{Re}[g^*(\theta)h(\theta)]/\sigma(\theta), \quad (8)$$

$$\beta(\theta) = \tan^{-1} \left(\frac{2 \operatorname{Im}[g(\theta)h^*(\theta)]}{|g(\theta)|^2 - |h(\theta)|^2} \right). \quad (9)$$

III. IMAGINARY POTENTIAL

In this section we discuss the form adopted for the imaginary potential. It is known^{6,7} that in principle the effective potential (optical potential) for the scattering of two nuclei is complex and nonlocal. This was discussed quite clearly in a paper by Benöhr and Wildermuth.⁷ In that paper it was shown how to derive a set of coupled integrodifferential equations for the various relative-motion wave functions appropriate to both scattering and reaction channels. With the use of Green's functions this set of equations can be formally reduced to a single integrodifferential equation which involves the relative-motion function in the elastic channel alone. This equation is the same as that obtained in the one-channel resonating-group calculation, except for the appearance of an additional nonlocal and non-Hermitian potential, characterized by a non-Hermitian integral kernel. In principle this additional kernel can be derived in

a microscopic manner; however, in general, this derivation will be so complicated that normally one would have to employ a phenomenological form in analyses of experimental data.

Although, as seen in Sec. II, we do not here adopt the procedure of introducing a phenomenological non-Hermitian kernel, the fact that in the formulation [Eq. (1)] we have allowed for a (J, l) dependence of the absorptive potential does mean that the possibility exists for accounting for non-local features of the imaginary part of the $p + \alpha$ effective potential. In fact, we here allow for a simple l dependence of the absorptive potential through the introduction of a Majorana component, which results in an odd-even orbital-angular-momentum dependence of the potential. The reasonableness of introducing nonlocality into the imaginary potential in such a simple manner is suggested by the following: (i) In a study of $n + \alpha$ scattering⁸ it was found that, in the Born approximation, the nonlocal features of the calculated potential can be exactly reproduced by using an equivalent potential containing a Majorana component but which is otherwise local; and (ii) in a study of $\text{He}^3 + \alpha$ scattering⁴ it was found that even at an energy where the Born approximation is not quantitatively valid, the calculated odd-even behavior of the real parts of the phase shifts can be reproduced reasonably well by a Majorana component

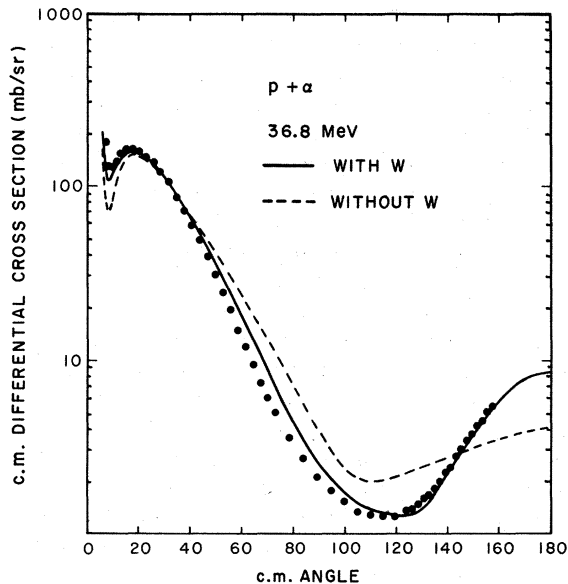


FIG. 2. Comparison of the present calculations with data (points) of Ref. 10 at a c.m. energy of 36.8 MeV. The dashed curve represents the calculation with no absorptive potential, and the solid curve represents the calculation with an absorptive potential having parameters $U_V=0$, $U_S=5.5$ MeV, $R=2.6$ F, $a=0.2$ F, and $C_I=-0.7$.

in the real effective potential. In addition, in this same study⁴ of $\text{He}^3 + \alpha$ scattering, the behavior of the imaginary parts of the phase shifts did suggest that it might be necessary to include a Majorana component in the imaginary potential.

The radial form for the absorptive potential is taken to be the commonly used Woods-Saxon-vol-

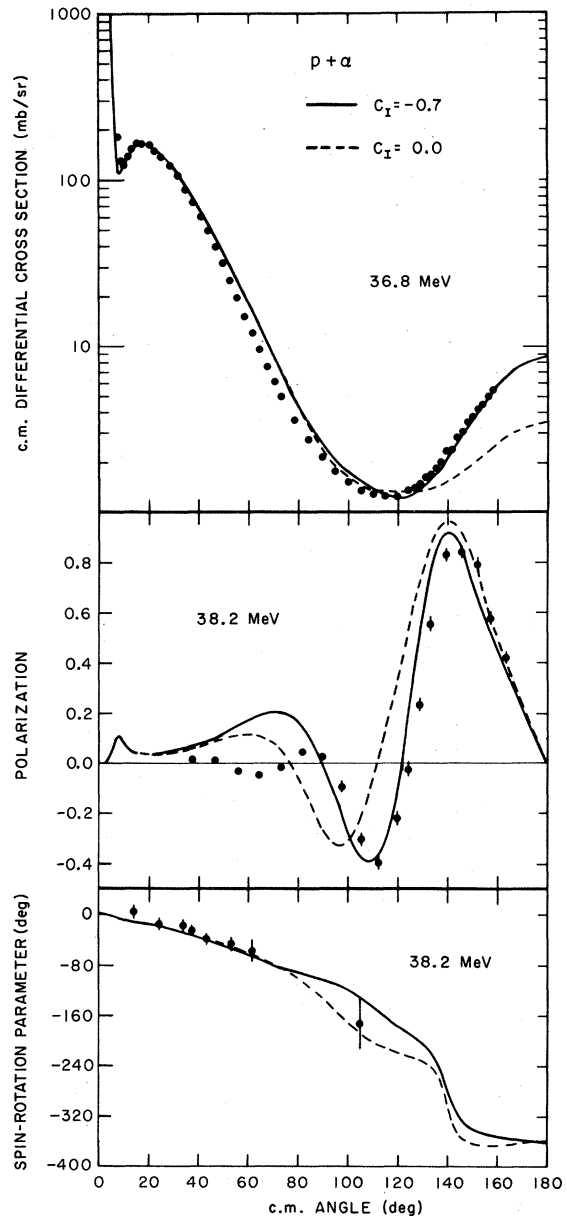


FIG. 3. Comparison of the present calculations with data (points) of Refs. 10-12 at the indicated c.m. energies. Equation (13) applies to both curves. The dashed curve represents a calculation with absorptive parameters $U_S=4.5$ MeV and $C_I=0$, and the solid curve represents a calculation with absorptive parameters $U_S=5.5$ MeV and $C_I=-0.7$. Both calculations yield a total reaction cross section of 86 mb.

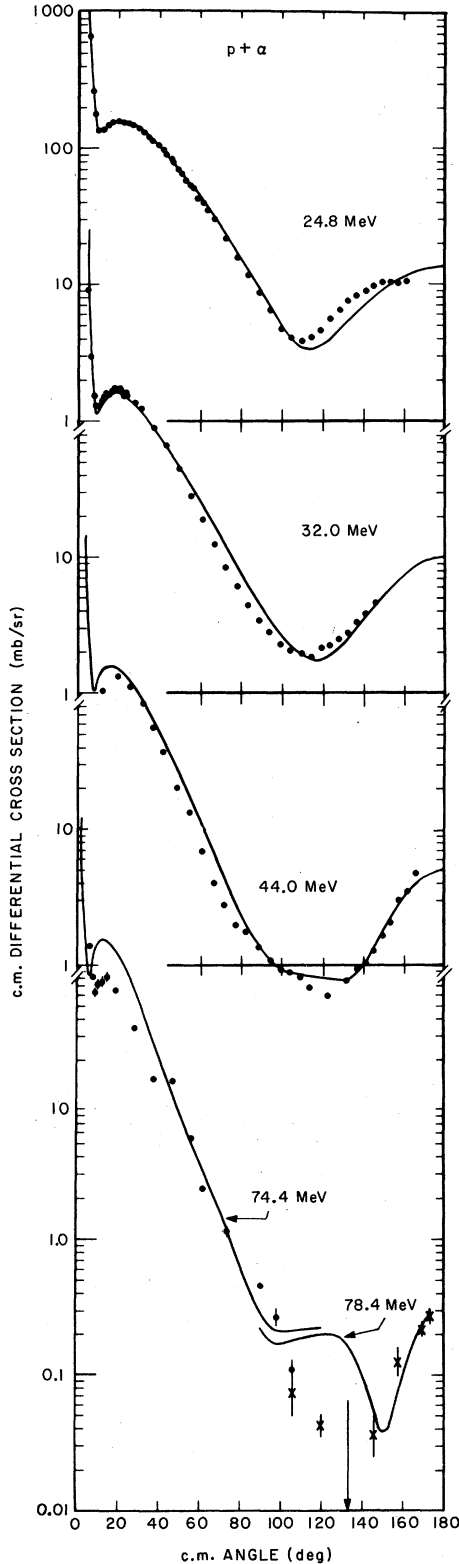


FIG. 4. Comparison of the present calculations (curves) with data (points) of Refs. 17-20 at the indicated c.m. energies. The absorptive parameters are given in Eq. (13) and Table I.

ume-plus-surface form. Such a form has been used in previous³⁻⁵ resonating-group studies of light systems. For simplicity, we choose the same radial form for the exchange component as for the nonexchange component of W . Therefore, we write

$$W = (1 + C_I P^r)U(r), \quad (10)$$

where

$$U(r) = \frac{-U_V}{1 + e^{(r-R)/a}} + \frac{-4U_S e^{(r-R)/a}}{[1 + e^{(r-R)/a}]^2}, \quad (11)$$

P^r is an operator which exchanges the space position of the proton with that of the c.m. of the α particle, and C_I is an adjustable parameter whose value is the strength of the exchange component of W relative to the nonexchange component. The potential of Eq. (10) results in the absorptive term in Eq. (1) being given by

$$W_{\pi}(r) \equiv W_i(r) = [1 + C_I(-1)^l]U(r). \quad (12)$$

IV. PROCEDURE AND RESULTS

There are seven constants in the nucleon-nucleon potential used in the present resonating-group calculations. The depth and range parameters of both the spin-singlet and spin-triplet components of the potential are chosen to yield correct values for the nucleon-nucleon effective-range parameters. These depths and range parameters are given in Eq. (7) of Ref. 1. The remaining three constants, which are the space-exchange parameter, and the depth and range parameter of the spin-orbit component of the potential, are chosen to yield an over-all good fit to $p+\alpha$ and $n+\alpha$ data below the reaction thresholds, with particular emphasis being given to the resonance behavior of the p -wave phase shifts. The values we use⁹ for these remaining three constants are those from Set III in Table I of Ref. 1.

With the above-described fixing of the constants in the nucleon-nucleon potential, the adjustable parameters available to fit the $p+\alpha$ data above the reaction threshold are those of the imaginary potential; i.e., U_V , U_S , R , a , and C_I of Eqs. (10) and (11). An extensive study was first undertaken using the 36.8-MeV differential-cross-section data of Bunker *et al.*,¹⁰ the 38.2-MeV polarization data of Craddock *et al.*,¹¹ and the 38.2-MeV spin-rotation-parameter data of Griffith *et al.*¹² The initial procedure we adopted for fitting this data was very similar to that used in previous studies.³⁻⁵ That is, U_S was set equal to U_V , the diffuseness parameter a was given the value 0.5 F, and the radius R was taken to yield an rms radius for the volume part of the absorptive potential nearly equal to that of the real direct nuclear po-

tential; that is $R = 2.25 F$. The effects of varying the two remaining parameters U_V and C_I were then investigated. With $C_I = 0$ and $U_V = 1.5$ MeV, the differential cross section is reproduced moderately well out to a c.m. angle of 120° , and the calculated total reaction cross section σ_R of 97 mb is reasonable.¹³ However, with $C_I = 0$ several types of discrepancy do exist: The calculated backward-angle differential cross section falls considerably below that found experimentally, the for-

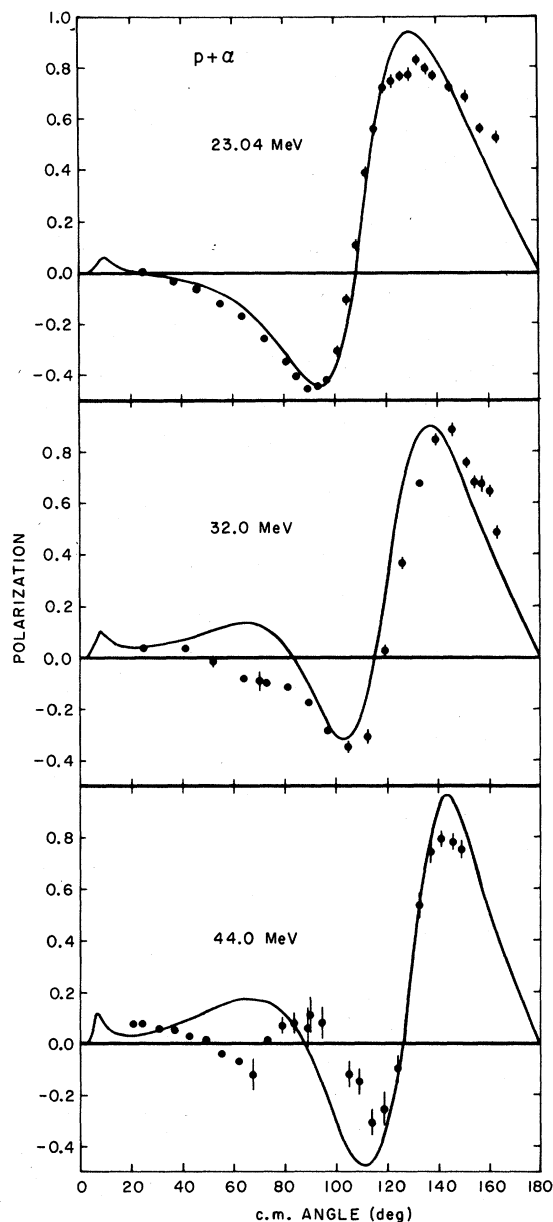


FIG. 5. Comparison of the present calculations (curves) with data (points) of Refs. 11 and 21 at the indicated c.m. energies. The absorptive parameters are given in Eq. (13) and Table I.

ward-angle polarization is calculated to be too large, and the 125° zero crossover of the polarization is calculated to occur at 108° instead. An adjustment of C_I can remove two of these discrepancies. A value $C_I = -0.7$ removes the discrepancies in the backward-angle differential cross section and in the 125° zero crossover of the polarization, while yielding only a small reduction in σ_R to 87 mb; however, the forward-angle polarization is still calculated to be too large. The dashed curve in Fig. 1 shows the resulting fit to the experimental differential cross section, polarization, and spin-rotation parameter.¹⁴ We should comment that the sign of C_I is well determined; thus positive values of C_I cause the above-discussed zero crossover of the polarization to move toward smaller angles rather than, as needed, toward larger angles, and such values of C_I do not improve the fit to the backward-angle differential cross section.

As has been mentioned, the choice of geometry parameters and the use of equal volume and surface absorption strengths in the above initial procedure are consistent with methods used previously in studies of other light systems.³⁻⁵ Next, a procedure was adopted of varying the geometry parameters and the ratio of volume to surface absorption in order to determine whether or not significant improvements could be made in the fits to the data of Fig. 1. Particular attention was paid to the question of an improvement in fit to the forward-angle polarization data. It was found that an increase in the strength U_S of the surface absorption relative to the strength U_V of volume absorption and a decrease in diffuseness a accompanied by an increase in radius R could serve to reduce the calculated forward-angle polarization while, in addition, marginally improving the over-all quality of the fit. We therefore decided to proceed with the analysis by using the fixed values

$$U_V = 0, \quad R = 2.6 F, \quad a = 0.2 F. \quad (13)$$

TABLE I. Absorptive parameters, U_S and C_I , and calculated total reaction cross sections σ_R at c.m. energies E of the present analysis. The absorptive potential is given by Eqs. (10) and (11) and the remaining parameters are given in Eq. (13).

E (MeV)	U_S (MeV)	C_I	σ_R (mb)
23.04	1.5	+0.20	36.7
24.8	2.5	-0.25	52.0
32.0	4.5	-0.70	72.9
36.8	5.5	-0.70	86.0
38.2	5.5	-0.70	85.8
44.0	5.5	-0.55	88.3
74.4	5.5	+0.20	75.7

The improvement in fit obtained is illustrated by the solid curve of Fig. 1, which is a curve calculated using Eq. (13), $U_s = 5.5$ MeV, and $C_I = -0.7$. It is especially notable that the same value of C_I is found here as was found in the initial procedure in spite of the quite different forms for the imaginary potential in the two cases. The total reaction cross section given by the present parameters is 86 mb, which is reasonable.¹³ The results that the absorption be of pure surface type and that the diffuseness be small are in agreement with the conclusions of Thompson *et al.*,¹⁵ who employed an 11-parameter¹⁶ optical model to analyze $p + \alpha$ data at c.m. energies from 24 to 44 MeV. In the remainder of the present work, Eq. (13) will be adhered to, and U_s and C_I will be adjusted at each energy to produce the best visual fit to the data.

The next two figures serve to indicate explicitly the need for an absorptive potential having a Majorana component. Figure 2 is a comparison of the experimental differential cross section at 36.8 MeV with calculations both with and without an absorptive potential. The figure presents a striking illustration of the need for an absorptive potential above the reaction threshold. Figure 3 compares

experimental data with calculations both with and without a Majorana component in the absorptive potential. The removal of the previously noted discrepancies in the differential cross section and polarization by the addition of a Majorana component is clearly demonstrated in the figure. In Figs. 4 and 5 we illustrate the best visual fits obtained at the remaining energies investigated. The differential-cross-section data are those of Bunch *et al.*,¹⁷ Brussel and Williams,¹⁸ Hayakawa *et al.*,¹⁹ and Selove and Teem.²⁰ The polarization data are those of Craddock *et al.*¹¹ and Boschitz *et al.*²¹ Table I lists the absorptive parameters U_s and C_I used in the present analysis and also gives the calculated total reaction cross section. Tables II and III list, respectively, the real parts and imaginary parts of the $p + \alpha$ phase shifts given by our calculation.

V. DISCUSSION AND CONCLUSIONS

The present fits were obtained with two energy-dependent parameters U_s and C_I . It is of interest to compare these fits to those reported by Thompson *et al.*,¹⁵ obtained with an 11-parameter¹⁶ optical model which contained a purely local imagi-

TABLE II. Real parts δ_{Jl}^R of the calculated $p + \alpha$ phase shifts δ_{Jl} , in degrees, at c.m. energies E of the present analysis.

l	J	E (MeV)						
		23.04	24.8	32.0	36.8	38.2	44.0	74.4
0	$\frac{1}{2}$	82.95	80.35	71.36	66.50	65.24	60.40	44.32
1	$\frac{1}{2}$	45.36	43.69	37.52	33.80	32.76	28.63	14.69
1	$\frac{3}{2}$	81.94	79.96	72.86	68.85	67.80	63.72	49.92
2	$\frac{3}{2}$	3.77	4.13	5.14	5.36	5.38	5.25	3.48
2	$\frac{5}{2}$	15.02	17.00	24.37	28.29	29.25	32.80	40.49
3	$\frac{5}{2}$	3.50	3.93	5.31	5.89	6.05	6.74	7.13
3	$\frac{7}{2}$	5.06	5.85	8.99	10.97	11.59	14.43	25.64
4	$\frac{7}{2}$	0.49	0.62	1.24	1.73	1.87	2.47	4.25
4	$\frac{9}{2}$	0.63	0.80	1.71	2.50	2.75	3.88	10.39
5	$\frac{9}{2}$	0.12	0.16	0.37	0.57	0.64	0.94	2.70
5	$\frac{11}{2}$	0.13	0.17	0.43	0.67	0.75	1.16	4.33
6	$\frac{11}{2}$	0.02	0.02	0.07	0.13	0.15	0.25	1.22
6	$\frac{13}{2}$	0.02	0.02	0.08	0.14	0.16	0.28	1.58
7	$\frac{13}{2}$	0	0	0.01	0.03	0.03	0.07	0.49
7	$\frac{15}{2}$	0	0	0.02	0.03	0.04	0.07	0.56
8	$\frac{15}{2}$	0	0	0	0.01	0.01	0.02	0.18
8	$\frac{17}{2}$	0	0	0	0.01	0.01	0.02	0.19

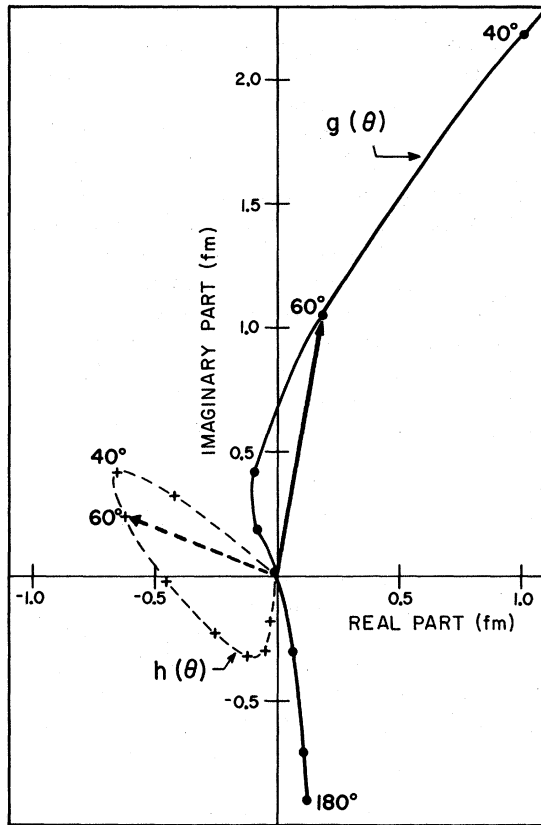


FIG. 6. Complex-plane representation of the calculated scattering amplitudes of Eqs. (2) and (3) at a c.m. energy of 38.2 MeV. The absorptive parameters used are given in Eq. (13) and Table I. The solid curve represents $g(\theta)$ and the dashed curve represents $h(\theta)$. The dots and crosses occur at c.m. angular intervals of 20° . The complex values of $g(\theta)$ and $h(\theta)$ at 60° are illustrated by the solid arrow and dashed arrow, respectively.

rors in ϕ when ϕ is near 90° .

The values of C_I determined from the present analysis are plotted vs energy in Fig. 7. The vertical bars are centered about the values of Table I, and the lengths of the bars indicate the range over which the C_I can be varied without causing a significant visual worsening of the fit to the data. The figure shows that, with the possible exceptions of the lowest-energy and highest-energy determinations, the values of C_I are negative, indicating a stronger absorption in odd-orbital-angular-momentum states than in even.

Although we feel that we have established here the need for a space-exchange term in the imaginary potential for the $p+\alpha$ system, we are presently not completely sure how to interpret the variation with energy of its relative strength C_I as exhibited in Fig. 7. We are currently studying the

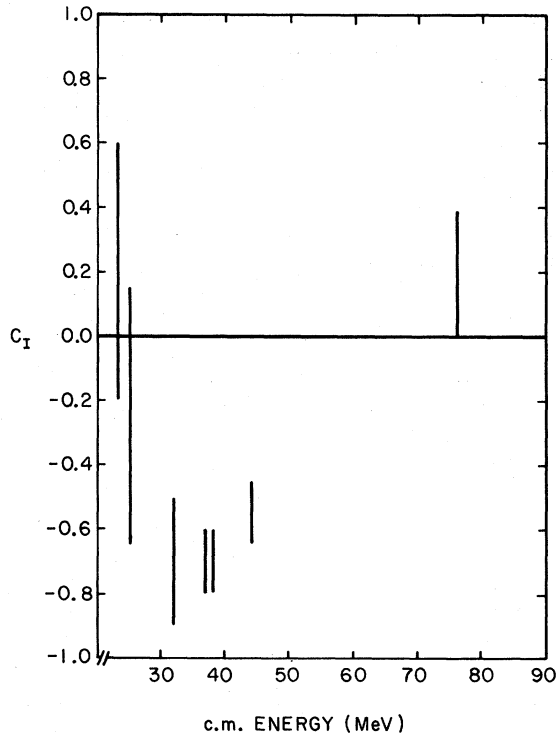


FIG. 7. The exchange parameter C_I of Eq. (10) vs energy, as determined from the present analysis. The vertical bars are centered about the values of Table I, and their lengths indicate the range over which C_I can be varied without causing the fit to the data to become visually worsened.

effect of including such an exchange term in the description of other light systems with the hope that understandable systematic features of C_I will be revealed.

In summary, we have fitted $p+\alpha$ differential-cross-section, polarization, and spin-rotation-parameter data between 23 and 75 MeV by incorporating a phenomenological imaginary potential into a treatment of the $p+\alpha$ system with the resonating-group method. In this fitting procedure we have used no free parameters in the real potential and two energy-dependent parameters in the imaginary potential. We have found the need for a space-exchange component in the imaginary potential, which indicates that at most energies the absorption is stronger in odd-orbital-angular-momentum states than in even. Thus it appears that the inclusion of a Majorana component in the imaginary potential may be a good way to account for some of the nonlocal features of this potential. Other light systems are currently being investigated with this in mind.

*Work supported in part by the U. S. Atomic Energy Commission. This is Report No. COO-1265-118.

¹I. Reichstein and Y. C. Tang, Nucl. Phys. **A158**, 529 (1970). In this Ref. there are two typographical errors in the Appendix. The error functions Φ which appear just after Eq. (A6) in the expression for the $p + \alpha$ Coulomb kernel should have arguments $(3\alpha/2)^{1/2}Q$ and $(3\alpha/2)^{1/2}Q'$.

²All energies refer to the c.m. system unless otherwise stated.

³R. E. Brown and Y. C. Tang, Nucl. Phys. **A170**, 225 (1971).

⁴Y. C. Tang and R. E. Brown, Phys. Rev. **C 4**, 1979 (1971).

⁵R. E. Brown, I. Reichstein, and Y. C. Tang, Nucl. Phys. **A178**, 145 (1971).

⁶H. Feshbach, Ann. Phys. (N.Y.) **5**, 357 (1958).

⁷H. C. Benöhr and K. Wildermuth, Nucl. Phys. **A128**, 1 (1969).

⁸D. R. Thompson and Y. C. Tang, Phys. Rev. **C 4**, 306 (1971).

⁹We have investigated the effects which an adjustment of these three constants have on the quality of the fits to the $p + \alpha$ data at energies above the reaction threshold. No significant improvement was produced by these adjustments; in particular the features produced by the Majorana component in the imaginary potential could not also be produced by the varying of these three constants.

¹⁰S. N. Bunker, J. M. Cameron, M. B. Epstein, G. Paic, J. R. Richardson, J. Rogers, P. Thomaš, and J. W. Verba, Nucl. Phys. **A133**, 537 (1969); and private communication from G. E. Thompson (see Ref. 15).

¹¹M. K. Craddock, R. C. Hanna, L. P. Robertsor, and B. W. Davies, Phys. Letters **5**, 335 (1963).

¹²T. C. Griffith, D. C. Imrie, G. J. Lush, and L. A. Robbins, Rutherford High Energy Laboratory Progress Report No. NIRL/R/81, 1964 (unpublished), p. 38.

¹³There are at present no very accurate measurements of σ_R . In some early cloud-chamber work, Tannenwald [P. E. Tannenwald, Phys. Rev. **89**, 508 (1953)] investigated $n + \alpha$ interactions produced by a neutron flux having a c.m. energy of 55 MeV at peak flux intensity and having an energy spread of about ± 2.5 MeV. He obtained

about 94 mb for σ_R ; however, 16 mb of this estimate is due to an unconfirmed conjecture about the number of undetected He³ tracks. Cairns *et al.* [D. J. Cairns, T. C. Griffith, G. J. Lush, A. J. Metheringham, and R. H. Thomas, in *Nuclear Forces and the Few Nucleon Problem*, edited by T. C. Griffith and E. A. Power (Pergamon, New York, 1960), Vol. II, p. 269] have reported an incomplete analysis of $p + \alpha$ interactions in a cloud chamber at a c.m. energy of 42.4 MeV. They estimate about 90 mb for σ_R . In Ref. 19, Hayakawa *et al.* report a study of $p + \alpha$ scattering and reactions at a c.m. energy of 44 MeV in which they used scintillation crystals and solid-state detectors. They obtain the very rough estimate for σ_R of from 50 to 80 mb.

¹⁴The angular range of the spin-rotation-parameter data is insufficient to be of much help in determining the parameters of the imaginary potential.

¹⁵G. E. Thompson, M. B. Epstein, and T. Sawada, Nucl. Phys. **A142**, 571 (1970).

¹⁶The model of Ref. 15 was, in effect, reduced to nine parameters when initial searches indicated that both the strength of the volume absorption and the strength of the imaginary spin-orbit term should be set equal to zero.

¹⁷S. M. Bunch, H. H. Forster, and C. C. Kim, Nucl. Phys. **53**, 241 (1964).

¹⁸M. K. Brussel and J. H. Williams, Phys. Rev. **106**, 286 (1957).

¹⁹S. Hayakawa, N. Horikawa, R. Kajikawa, K. Kikuchi, H. Kobayakawa, K. Matsuda, S. Nagata, and Y. Sumi, J. Phys. Soc. Japan **19**, 2004 (1964); and private communication from G. E. Thompson (see Ref. 15).

²⁰W. Selove and J. M. Teem, Phys. Rev. **112**, 1658 (1958).

²¹E. T. Boschitz, M. Chabre, H. E. Conzett, E. Shield, and R. J. Slobodrian, in *Proceedings of the Second International Symposium on Polarization Phenomena of Nucleons, Karlsruhe, Germany, 1965* (Birichäuser, Basel, Switzerland, 1966), p. 328; and private communication from G. E. Thompson (see Ref. 15).

²²See Refs. 3-5. Note, however, that these previous studies did not include noncentral components in the nucleon-nucleon potential.

Induced-Tensor and Second-Order-Forbidden Terms*

Barry R. Holstein

Department of Physics and Astronomy, University of Massachusetts, Amherst, Massachusetts 01002

(Received 6 March 1972)

A model-independent result for the β - γ correlation in allowed β decay is given, including all second-order-forbidden corrections. A suggested method for measurement of the first-class contribution to the induced-tensor form factor is discussed.

I. INTRODUCTION

Recently, we have reported predictions for contributions to the induced-tensor term d_1 in allowed

nuclear β decay which arise from the conventional (first-class) axial-vector current.¹ Of course, if second-class axial currents² contribute to the semileptonic weak decays, as suggested by one